

Concurrent Harvesting of Ambient Energy by Hybrid Nanogenerators for Wearable Self-Powered Systems and Active Remote Sensing

Haiwu Zheng,^{†,‡,§,#} Yunlong Zi,^{†,§,#} Xu He,^{†,§,#} Hengyu Guo,^{†,||} Ying-Chih Lai,[†] Jie Wang,^{†,||} Steven L. Zhang,[†] Changsheng Wu,[†] Gang Cheng,^{†,§} and Zhong Lin Wang^{*,†,||}

[†]School of Materials Science and Engineering, Georgia Institute of Technology, Atlanta, Georgia 30332-0245, United States

[‡]Henan Key Laboratory of Photovoltaic Materials, School of Physics and Electronics and [§]Key Lab for Special Functional Materials, Ministry of Education, Henan University, Kaifeng 475004, China

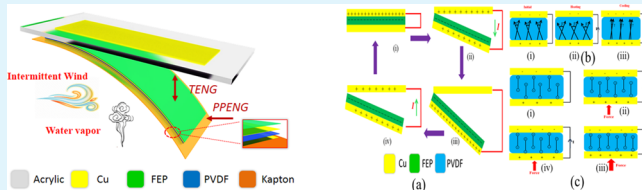
^{||}Beijing Institute of Nanoenergy and Nanosystems, Chinese Academy of Sciences, Beijing 100083, China

[#]Department of Mechanical and Automation Engineering, The Chinese University of Hong Kong, Shatin, N.T., Hong Kong SAR, China

S Supporting Information

ABSTRACT: Harvesting energy available from ambient environment is highly desirable for powering personal electronics and health applications. Due to natural process and human activities, steam can be produced by boilers, human perspiration, and the wind exists ubiquitously. In the outdoor environment, these two phenomena usually exist at the same place, which contain heat and mechanical energies simultaneously. However, previous studies have isolated them as separate sources of energy to harvest and hence failed to utilize them effectively. Herein, we present unique hybrid nanogenerators for individually/simultaneously harvesting thermal energy from water vapors and mechanical energy from intermittent wind blowing from the bottom side, which consist of a wind-driven triboelectric nanogenerator (TENG) and pyroelectric–piezoelectric nanogenerators (PPENGs). The output power of the PPENG and the TENG can be up to about 184.32 μ W and 4.74 mW, respectively, indicating the TENG plays the dominant role. Our hybrid nanogenerators could provide different applications such as to power digital watch and enable self-powered sensing with wireless transmission. The device could also be further integrated into a face mask for potentially wearable applications. This work not only provides a promising approach for renewable energy harvesting but also enriches potential applications for self-powered systems and wireless sensors.

KEYWORDS: triboelectric nanogenerator, piezoelectric nanogenerator, pyroelectric nanogenerator, energy harvesting, wearable device



1. INTRODUCTION

Our surroundings have plentiful energy resources in various forms, among them the most common is solar energy, which can be completely harvested under the full sun. However, harvesting of solar energy could be affected by the weather. Especially on cloudy days or at night, the output of solar cell is enormously restrained or even disappeared.^{1,2} Therefore, it is imperative to investigate other forms of energy, such as mechanical energy (wind, vibration) and waste thermal energy (vapor, breathing). Mechanical energy, one of the most ubiquitously available energies in the environment, has been used for long term by converting itself into electrical energy via generators, such as electromagnetic generator,^{3–5} piezoelectric nanogenerator (PiENG),^{6–8} and triboelectric nanogenerator (TENG).^{9–14} Among them, TENG has exhibited lots of advantages such as low cost, environmental friendless, ample choices of materials, and so on.^{15,16} PiENG can be used to harvest mechanical energy through the deformation of piezoelectric materials, which usually exhibits pyroelectric effect

for thermal energy harvesting. Due to natural processes and human activities, the steam (vapors) can be produced by some items such as boilers, heating pipes, human perspiration, and the wind exists ubiquitously. In the outdoor environment, these two phenomena usually abundantly exist at the same place, which contain heat and mechanical energies simultaneously.¹⁷ However, previous studies have isolated them as separate sources of energy to be harvested and hence failed to utilize them effectively. At the same time, it has been reported that intermittent wind could improve the capture efficiency of water vapor.¹⁸ Thus, it is very reasonable for us to design hybrid nanogenerators to collect wind and heat energy synchronously, forming an integrated hybrid energy harvesting system.

The flutter-based TENG has been developed to effectively harvest mechanical energy in wind.^{19,20} However, the strain

Received: January 28, 2018

Accepted: April 16, 2018

Published: April 16, 2018

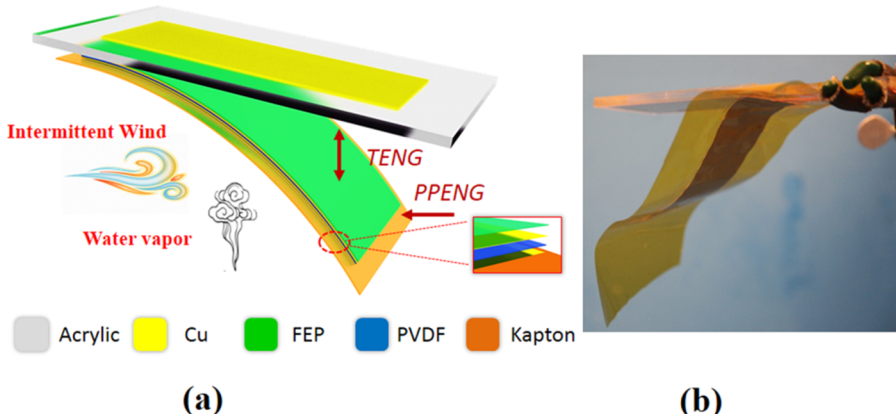


Figure 1. Hybrid nanogenerators. (a) Schematic illustration of the hybrid nanogenerators. (b) The optical image of as-prepared hybrid nanogenerators.

energy brought by the wind-driven deformation of the flutter and the thermal energy in the temperature fluctuation have not been utilized. On the other hand, ferroelectric poly(vinylidene fluoride) (PVDF), a kind of flexible ferroelectric polymer, could be utilized not only in the scavenging of mechanical energy through piezoelectric effect but also in the harvesting of thermal energy.^{21,22} Therefore, it is highly desirable to realize the simultaneous collection of the additional mechanical and thermal energies through rational design of the device based on PVDF.

In this work, we constructed a hybrid nanogenerator that can concurrently or independently harvest thermal energy from water vapors and mechanical energy from intermittent wind blowing from the bottom side. The hybridized nanogenerators are based on wind-driven TENG and pyroelectric–piezoelectric nanogenerators (PPENGs). Compared to the TENG or the PPENG, the hybridized nanogenerators have much better charging performance for a $22\ \mu\text{F}$ capacitor. The hybrid nanogenerators have been demonstrated to power light-emitting diodes (LEDs) and a commercial digital watch with the calculation function. The device can also be used as a self-powered sensor for wind speed. This work renders an effective solution to harvest ambient thermal and mechanical energies for wearable self-powered systems and active remote sensing.

2. EXPERIMENTAL SECTION

2.1. Fabrication of the Hybrid Nanogenerators. First, a rectangular acrylic sheet ($300\ \text{mm} \times 90\ \text{mm} \times 3.175\ \text{mm}$) served as supporting substrate was processed by laser cutting (PLS6.75, Universal Laser Systems). Then, a copper film was deposited on a fixed acrylic board as the top electrode. A commercially available polarized PVDF film with a thickness of $52\ \mu\text{m}$ deposited by Cu film layers on both sides was selected to construct PPENG. The four corners of rectangular PVDF film with size of $11.5\ \text{cm} \times 5\ \text{cm}$ were carefully pasted to one side of Kapton film ($500\ \text{mm} \times 160\ \text{mm} \times 0.0254\ \text{mm}$) through the Kapton tape to ensure it is flat at the surface, whereas another side of Kapton film faces wind and/or water vapors directly. The larger area of Kapton film is to keep triboelectric surfaces of TENG isolated from vapors. A single-sided sticky fluorinated ethylene propylene (FEP) film with a thickness of $52\ \mu\text{m}$ was applied to totally cover the PVDF film. The FEP film is used as the top surface of the flutter, and the PVDF film attached on the Kapton film is set to the bottom part of the flutter. One end of the flutter is fixed on the side of the acrylic board, leaving the other side free-standing. Two lead wires were respectively connected to metal Cu electrode.

2.2. Fabrication of the Small-Scale Hybrid Nanogenerators. For the demonstration of face mask, a polarized PVDF film ($52\ \mu\text{m}$ in

thickness, $7.0\ \text{cm}$ in length, and $3.2\ \text{cm}$ in width) completely covered by a single-sided sticky FEP film ($52\ \mu\text{m}$ in thickness) was carefully pasted to one side of the rectangular Kapton film ($52\ \mu\text{m}$ in thickness) with a larger area than that of the FEP film. To easily match the face mask and with the aim of contacting and separation, two sides of the Kapton film were stuck to the stripped acrylic board to form an arc shape with a height of $5\ \text{mm}$.

2.3. Electrical Measurement. The signals of output voltage, output current, and short-circuit transferred charges for the devices were measured by a preamplifier (Keithley 6514 system electrometer), and the temperature was recorded by an infrared camera (FLIR C2). The software platform was constructed using LabVIEW, which was capable of realizing real-time data collection and analysis.

3. RESULTS AND DISCUSSION

The hybrid nanogenerators illustrated in Figure 1a mainly consist of two parts, a wind-driven TENG part and a PPENG part. The flutter-driven TENG design was employed for wind energy harvesting. A copper film was deposited on a fixed acrylic board as the top electrode and one triboelectric surface. A $52\ \mu\text{m}$ thick FEP film was used on the top of the flutter, as the other triboelectric surface. One end of the flutter was fixed on the side of the acrylic board, leaving the other side free-standing. During contact–separation process between the FEP film and top copper electrode as driven by intermittent wind, periodic alternative current (AC) output could be delivered via TENG based on the coupling between triboelectrification and electrostatic induction. That is to say, the intermittent wind provides a driving force for the TENG work. As shown in Figure 1a, the direction of intermittent wind is almost parallel to the plane of the acrylic board substrate. To harvest the thermal energy brought by the temperature variation via pyroelectric effect and the strain energy brought by bending and torsion of the flutter via piezoelectric effect, a PPENG, with a $52\ \mu\text{m}$ thick PVDF film as functional material, was fabricated as the bottom part of the flutter. The temperature variation was induced by condensation process, during which water vapors were converted to droplets, and evaporation process of water droplets due to the intermittent wind.¹⁸ The bottom copper electrode of TENG was shared with the PPENG as the top electrode. Another copper film was deposited on the bottom surface of PVDF as the other electrode of the PPENG. A Kapton film was attached below PPENG to keep triboelectric surfaces of TENG isolated from water vapors. The area of the hybrid nanogenerators is $11.5\ \text{cm} \times 5\ \text{cm}$, and the maximum displacement of the flutter is about $6\ \text{cm}$. Through this rational

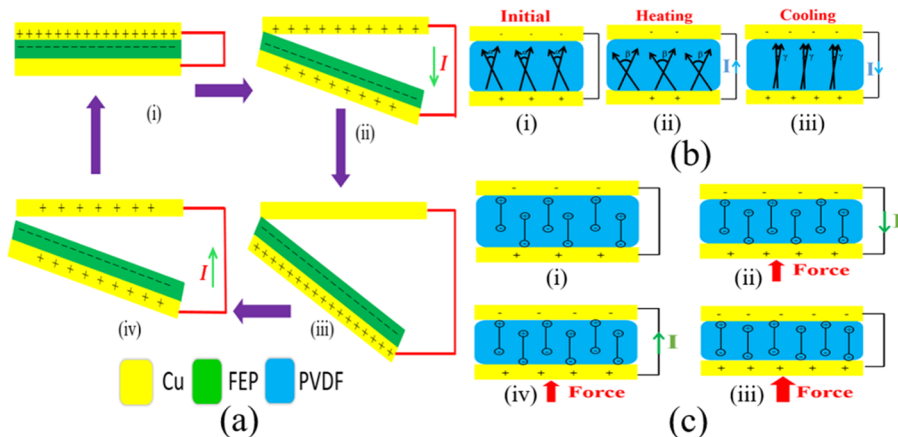


Figure 2. (a) Schematic sketch of the working principle of the TENG in hybrid cell. (b) The working mechanism of pyroelectric output in the PPENG. The magnitude of angle β is larger than that of the α , and the magnitude of angle γ is smaller than that of the α . (c) Schematic diagram of the working mechanism of piezoelectric nanogenerator in the PPENG to produce electricity.

design, the mechanical energy in the wind and the thermal energy in water vapors can be effectively harvested simultaneously or independently. The flutter of the hybrid nanogenerators is hung below the acrylic board, as indicated by the optical image of the hybrid nanogenerators in Figure 1b.

The operation and theoretical investigations of the contact–separation mode TENG have been carried out previously.^{23–25} Figure 2a displays the working mechanism of the TENG part in the hybrid nanogenerators. The wind-driven fluttering results in the relative contact–separation motion between the FEP film and the Cu film deposited on the acrylic board. Here, the Cu film plays dual roles as a triboelectric surface and as a top electrode of the TENG. Once the FEP film is in physical contact with the top Cu electrode, the surface of FEP gets negatively charged (Figure 2a-i), whereas the top Cu layer is positively charged owing to contact electrification governed by their different triboelectric polarities.²⁶ The negative charges on the FEP are immobile and are inclined to retain for a long time in view of insulating property of the electret polymer. As the FEP is separating away from the top Cu layer when the intermittent wind stops (Figure 2a-ii), a potential will be produced between the two electrodes of the TENG. Under short-circuit condition, the electrostatic induction by the negative FEP drives the electron flows from the middle Cu electrode to top Cu electrode through external circuit to balance out the charge distribution between the two electrodes in the TENG, generating an output current pulse from the top electrode to the bottom electrode in the TENG,^{27,28} until the FEP film in the flutter fully separates away with the top of the Cu film (Figure 2a-iii). When the FEP approaches the top Cu layer again driven by the intermittent wind, the negative surface charges in the FEP promote free electrons back to bottom electrode of TENG, yielding a pulsed current with opposite direction (Figure 2a-iv). Therefore, the wind-driven reciprocating motion of the flutter will generate AC pulse between the two electrodes in the TENG.

To elucidate the mechanism from thermal energy to electrical energy, a schematic sketch is shown in Figure 2b, based on the thermally induced random dithering of the electric dipole near its equilibrium axis. No output current can be found if the spontaneous polarization in PVDF is constant under invariable temperature, as described in Figure 2b-i. When the flutter meets the hot water steam, the temperature of the PVDF

film will be enhanced rapidly. Meanwhile, the aligned electric dipoles oscillate within a larger degree of spread around their respective aligning axes, which reduce the total average spontaneous polarization density.^{29,30} To balance the extra charges due to the decrease of polarization density, a current is driven to flow from the bottom electrode to the top electrode of the PVDF, as revealed in Figure 2b-ii. Conversely, when the PVDF is cooled, the polarization will be significantly enhanced because the electric dipoles oscillate within a smaller degree of spread angles due to less active thermal action, resulting in an increase in the amount of induced charges in the Cu electrodes of the PVDF.³¹ On this occasion, the current flows in the opposite direction, as indicated in Figure 2b-iii.

Figure 2c shows the power generation diagram based solely on piezoelectric effect of the PPENG. The working principle of the PiENG is derived from insulating property of the PVDF and the creation of an inner piezoelectric field during the applied strain. In the absence of any strain, the output current from the piezoelectric effect is zero, as presented in Figure 2c-i. When the intermittent wind blew the flutter, the impact between the acrylic board and the flutter was produced, which caused a compressed/stretched strain on the poled PVDF film. Consequently, the total spontaneous polarization of the PVDF was increased and the current flowed from the top to the bottom electrode in the PPENG to balance the extra polarization density¹⁷ (Figure 2c-ii). In the instant contact between the flutter and the top Cu electrode, the largest force was accomplished (Figure 2c-iii). On the other hand, the current flows back when the flutter begins to separate from the acrylic board and the strain releases (Figure 2c-iv). During the charging and discharging process, the PVDF acts like a “charge pump”, which drives electrons flow back and forth through the external circuit, leading to an AC electricity output. In contrast with the pyroelectric effect, the piezoelectric effect is more complex for the reason that all of the three-dimension strains could affect the polarization.²⁷

The output performance of the hybrid nanogenerators is systematically characterized with the simulated intermittent wind and water vapor environments. The electrical output of each part (TENG, PiENG, and PPENG) is first measured. To investigate the output performance of TENG for scavenging wind energy, a wind faucet in our lab is used to simulate the natural wind, which is employed as wind source with tunable

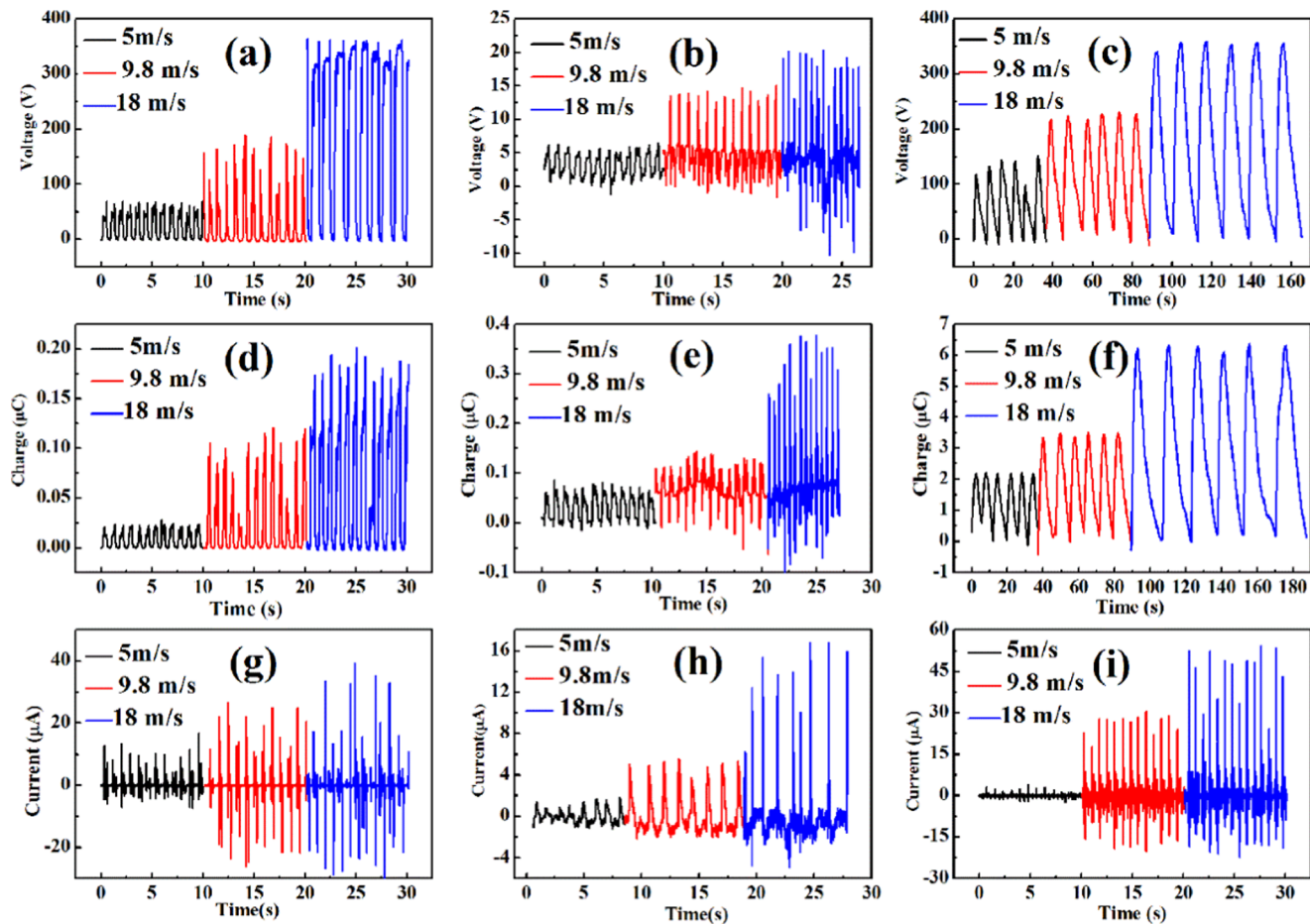


Figure 3. Output performances of the hybrid nanogenerator, including (a–c) open-circuit voltage, (d–f) short-circuit transfer charge, and (g–i) short-circuit current of triboelectric, piezoelectric, and PPENG outputs.

flow speed. Figure 3a depicts open-circuit voltage (V_{oc}) of the TENG as a function of wind speed ranging from 5 to 18 m/s. The results indicate that the V_{oc} increases with increasing wind speed with the maximum value of about 350 V at 18 m/s, which matches with the literature reports.^{24,32} As shown in Figure 3d, the short-circuit transfer charge (Q_{sc}) of the TENG has the same variation trend as the V_{oc} with increasing wind speed, which can reach 0.15–0.2 μ C at 18 m/s. The solely piezoelectric output for the PPENG device is measured with simulated wind and without water vapor. As presented in Figure 3b,e, the V_{oc} and Q_{sc} of the piezoelectric output apparently enhance with the increase of wind velocity, and the highest values of the V_{oc} and Q_{sc} can reach approximately 20 V and 0.3–0.4 μ C at 18 m/s, respectively. The V_{oc} value originated from the piezoelectric effect in this work is comparable to or higher than other PVDF-based piezoelectric nanogenerator,^{6,33,34} considering that the deformation of the flutter driven by the wind is even larger. The PPENG output was measured when both of the intermittent wind and water vapors worked simultaneously. The water vapor is simulated by an electric kettle. As expected, the V_{oc} and Q_{sc} of the PPENG output improve as the wind speed enhances (Figure 3c,f). Moreover, it can be found that the output performance under the synergistic actions of pyroelectric and piezoelectric effect is larger than that of solely piezoelectric effect, from which the maximum values of the V_{oc} and Q_{sc} were measured to be about 350 V and 6 μ C, respectively. To measure the pyroelectric coefficient accurately and exclude the influence of piezoelectric

output, we completely fixed flutter by tapes to avoid deformation of the PVDF film. As indicated by a thermal imaging system, the corresponding temperature variation can be about 25–50 °C, and the pyroelectric coefficients at different wind velocities are estimated to be 1.59 ± 0.19 , 1.91 ± 0.07 , and 2.64 ± 0.15 nC/(cm² K) at different wind speeds of 5, 9.8, and 18 m/s, respectively, which is consistent with previously reported values.^{27,35} Details of the calculation of pyroelectric coefficients for the PVDF film at different wind velocities is shown in Figure S1 in the Supporting Information. For the hybrid nanogenerators working concurrently with simulated wind and water vapors, the short-circuit current (I_{sc}) outputs were measured up to ~29 μ A for TENG and ~41 μ A for PPENG, as shown in Figure 3g,i. The piezoelectric I_{sc} from PiENG could achieve 14 μ A, which was obtained via the deformation of PVDF under only the wind, as indicated in Figure 3h. The corresponding short-circuit current densities from TENG, PiENG, and PPENG are ~5.05, 2.44, and ~7.13 mA/m², respectively.

The relationship between the effective output power and the resistance of external load is an important characteristic of the nanogenerators. The instantaneous power outputs versus the external load resistances at different wind velocities for TENG output, PiENG only, and PPENG output are drawn in Figure 4a–c,d–f,g–i, respectively, wherein the output power (P) was calculated by $P = I^2R$, where I is the output current and R is the loading resistance. To determine the optimized load resistance and the maximum instantaneous power of the TENG, the

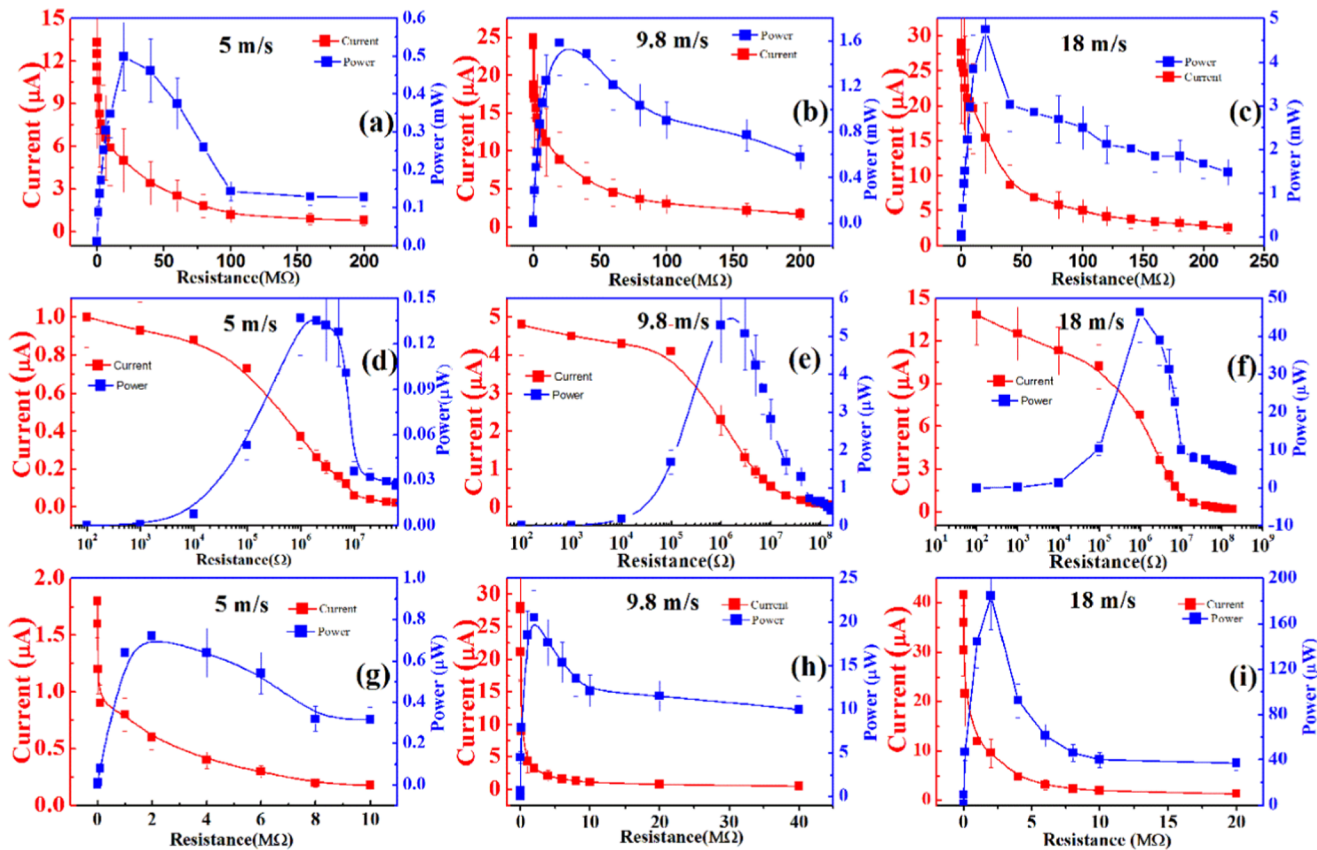


Figure 4. Peak power outputs vs the external load resistances for (a–c) TENG output only, (d–f) piezoelectric output only, (g–i) PPENG output with wind speeds of 5 m/s (left column), 9.8 m/s (middle column), and 18 m/s (right column).

Table 1. Optimized External Load and Peak Maximum Power Output for Each Part of Outputs under Different Wind Speeds

wind speed	5 m/s	9.8 m/s	15 m/s
piezoelectric output	1 MΩ, (0.14 ± 0.03) μW	1 MΩ, (5.29 ± 1.01) μW	1 MΩ, (46.24 ± 7.86) μW
TENG output	20 MΩ, (0.5 ± 0.09) mW	20 MΩ, (1.58 ± 0.28) mW	20 MΩ, (4.74 ± 0.71) mW
piezo + pyro output	2 MΩ, (0.72 ± 0.13) μW	2 MΩ, (20.48 ± 3.07) μW	2 MΩ, (184.32 ± 29.49) μW

relationship between output current and external load resistances was measured. As displayed in Figure 4c, the largest instantaneous output power of TENG attains approximately 4.74 mW with a load resistance of 20 MΩ, which is comparable to two other literatures.^{32,36} Larger wind velocity makes faster vibration of the flutter and facilitates fully contact and separation between the Cu and the FEP, which are beneficial for the enhancement of output power of the TENG. For the piezoelectric output, the current drops with the increase of load resistance at a low wind speed (5 m/s), as indicated in Figure 4d. The corresponding instantaneous power initially increases in the resistance region from 10² to 10⁶ Ω and then descends at higher external resistances (from 10⁶ to 6 × 10⁷ Ω). As a result, the instantaneous power reaches a maximum value of about 0.14 μW under a load resistance of 1 MΩ, as shown in Table 1. Moreover, the instantaneous piezoelectric output power increases with the increasing wind velocity, from which the maximum value is about 46.24 μW at a large wind velocity (18 m/s), as shown in Figure 4f. The piezoelectric output power in this work is almost consistent with that of piezoelectric nanogenerator based on PVDF.^{37–39} Larger wind velocity can induce the greater deformation of the PVDF, which are favorable to boost the piezoelectric output power. The variation trend of maximum output power with wind velocity for the

piezoelectric output is similar to that of the triboelectric output. With respect to the PPENG output, it is found that the instantaneous output power reaches the maximum value of 20.48 μW under a load resistance of 2 × 10⁶ Ω at a wind speed of 9.8 m/s (Figure 4h), and the instantaneous output power of the PPENG at the same load resistance enhances with the increase of wind velocity (Figure 4g–i). In addition, as seen from Figure 4i and Table 1, the maximum output power for the PPENG is 184.32 μW at a wind speed of 18 m/s, which is relatively lower than that of the TENG at the same wind velocity. This means that the TENG plays a dominant role in the total power output of the hybrid nanogenerators, whereas the PPENG serves as a complementary power source to harvest additional mechanical energy and the thermal energy. The overall power output could be up to ~5 mW under a wind speed of 18 m/s.

As demonstrated previously,²⁷ in a hybrid cell, the piezoelectric and pyroelectric outputs are usually effective to enhance the charging rate during energy storage. Here, we demonstrated the enhanced charging rate to a 22 μF capacitor brought by the PPENG output. As indicated in Figure 5a, the TENG and PPENG were electrically connected with three pairs of diodes, which functioned as rectifiers in altering the AC output signals of the nanogenerators to direct signals for charging commercial

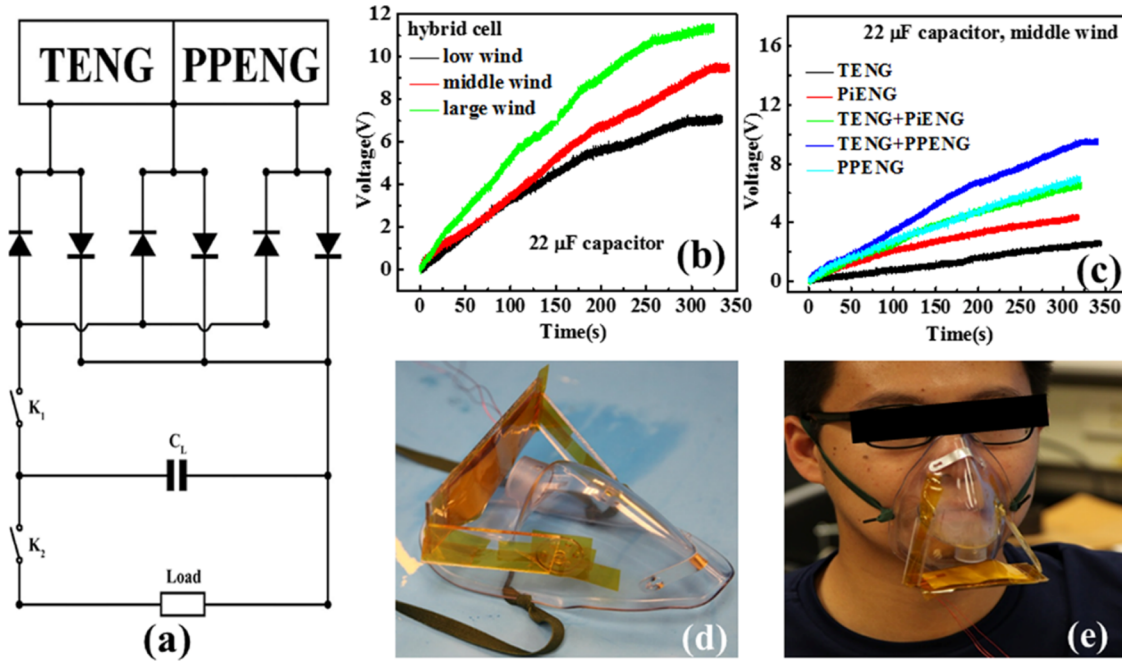


Figure 5. (a) Circuit diagram to hybridize the outputs from TENG and PPENG. (b) The charging curves of the $22\ \mu\text{F}$ capacitor by using the hybrid nanogenerators under different wind velocities. (c) The measured voltage of the $22\ \mu\text{F}$ capacitor charged by TENG, PiENG, TENG + PiENG, PPENG, and TENG + PPENG. (d) The integrated hybrid nanogenerator in the face mask and (e) the demonstration to wear the device.

capacitors. When K₁ is switched on and K₂ is switched off, the commercial capacitor is charged by the hybrid nanogenerators. When both K₁ and K₂ are turned on, the hybrid nanogenerators could sustainably drive some loads, such as a digital temperature–humidity meter and white LED lights. Figure 5b shows the overall charge profile of the hybrid nanogenerators under low (5 m/s), middle (9.8 m/s), and large (18 m/s) wind speeds. It was found that the charging rate increased with increasing wind speed, which was related to the larger power output at higher wind speed. For a large wind speed of 18 m/s, the voltage of the capacitance could reach 11 V in 300 s of charging. As shown in Figure 5c, through 300 s of charging under middle wind speed using the TENG output only, the voltage only reaches ~ 2.3 V. The voltage could ramp up to ~ 4.1 V within 300 s by the PiENG output solely, whereas the voltage will reach ~ 6.3 V within 300 s charged by the TENG and the PiENG outputs simultaneously. The voltage will also achieve ~ 6.3 V in 300 s when the PPENG was used to charge the $22\ \mu\text{F}$ capacitor. The overall outputs from all parts of the hybrid nanogenerators operated at middle wind speed can charge the capacitor to be ~ 9 V within 300 s. Therefore, it is obvious that hybrid nanogenerators have much better charging performance compared to those of individual TENG, PiENG, PPENG, or TENG + PiENG. With the output from the PPENG, the total enhancement of the charging rate brought by the hybrid nanogenerators could be almost 3 times. In addition, the stability of the TENG was also characterized by the long-term cycles, as shown in Figure S2. It is seen that about 5% of electrical output degradation was observed after continuous operation of ~ 6000 cycles (for 90 min). The good robustness satisfies the needs of reliability for practical nanogenerators under harsh environments.

With the enhanced power output and the charging rate, we have demonstrated several applications of these hybrid nanogenerators for powering electronics and wearable devices, self-powered sensing and wireless transmissions.^{40,41} By

harvesting the energies from the simulated wind and water vapors, the output of the hybrid nanogenerators was utilized to successfully light up 24 small white LEDs (Video 1, Supporting Information). With rectifiers used and a capacitor as the temporary energy storage device, the hybrid nanogenerators can also be used to power a commercial watch with the calculation function (Video 2, Supporting Information) and to drive the operation of a commercial digital temperature–humidity meter (Video 3, Supporting Information). Considering that the outputs of the hybrid nanogenerators are related to the wind speed, the device can also be used as a self-powered sensor for the wind speed. Here, it is noticed that the microcontroller systems of transmitter and receiver were powered by batteries, and the hybrid nanogenerators (only TENG + PiENG outputs from the mechanical energies) were employed as active sensors. A commercially available wireless transmission circuit is integrated to transmit the detected wind speed to the computer, displayed as the corresponding numbers in the monitor (Video 4, Supporting Information). The wind speed, varied from 6 to 18 m/s, can be detected using the hybrid nanogenerators. In addition, to make this device wearable, we modified the design of the device and integrated it into a face mask so that the energies in the hot air exhaled by the human mouth can be effectively harvested by means of triboelectric, piezoelectric, and pyroelectric effect to power wearable electronics and biomedical sensors, which can reflect the breathing status of human being and thus monitor human health.⁴² When exhaling, the moist and warm airflow released by human breathing will bring thermal energy to the PVDF film, in which the dipole moments will be reduced, resulting in output electricity due to pyroelectric effect. Moreover, the arclike structure of the device makes it easier for the deformation of PVDF and periodic contact and separation between the FEP and Cu film, which can also generate electricity in virtue of piezoelectric and triboelectric effects. Figure 5d shows the photograph of the device integrated with

the face mask, which is wearable to harvest energies during the breath of human (Figure 5e). By using the normal human breath, 31 green LED bulbs are lighted concurrently, which testified the capability of the integrated hybrid nanogenerators for self-powered applications (Video 5, Supporting Information). The open-circuit voltage, short-circuit transferred charge, and short-circuit current from TENG and PPENG performances for the specially designed face mask device driven by the respiration of a young man could be found in Figures S3a–c and S4a–c, respectively, in the Supporting Information. The specially designed face mask device offers a good application prospect in the scope of self-powered healthcare monitoring, such as breathing and temperature sensors of human body and human respiratory rates.⁴³

4. CONCLUSIONS

In summary, we have devised and integrated triboelectric–pyroelectric–piezoelectric hybrid nanogenerators to effectively harvest energies from the wind and the water vapor, which are both abundance in the ambient environment. Each unit of TENG, PiENG, and PPENG could be utilized to individually or simultaneously scavenge the mechanical and thermal energies. The hybrid device takes advantage of its two or three constituent parts, which brings about a higher power output as compared to that from each individual nanogenerator. Hundreds of volts in output voltage and tens of microampere in output current are measured, with a maximized output power of ~5 mW. The hybridization of the PPENG into the TENG has been demonstrated to enhance the charging rate to a 22 μF capacitor by almost 3 times. In addition, the hybrid nanogenerators can power LEDs, a digital watch with calculator function and enable self-powered sensing with wireless transmission. The device was further integrated into a face mask for potentially wearable applications. This work will promote an important step toward hybridized energy harvesting in these situations where the airflow and temperature variations concurrently exist, such as human respiration, heating pipe, or boilers.

■ ASSOCIATED CONTENT

S Supporting Information

The Supporting Information is available free of charge on the ACS Publications website at DOI: [10.1021/acsami.8b01635](https://doi.org/10.1021/acsami.8b01635).

Test results of temperature oscillation patterns and short-circuit transfer charge for the pyroelectric nanogenerator at different wind speeds, the electrical performance of the small-scale hybrid nanogenerators (TENG + PPENG) by human respiratory (PDF)

Demonstration of successfully lighting up 24 small white LEDs (AVI)

Demonstration of the self-powered electronic watch (AVI)

Demonstration of the self-powered digital temperature–humidity meter (AVI)

Demonstration of a wireless transmission circuit to detect wind speed (AVI)

Demonstration of powering 31 green LED bulbs using the normal human breath (AVI)

■ AUTHOR INFORMATION

Corresponding Author

*E-mail: zhong.wang@mse.gatech.edu. Phone: (404) 894-8008. Fax: (404)894-9140.

ORCID ®

Haiwu Zheng: [0000-0002-2021-4159](https://orcid.org/0000-0002-2021-4159)

Yunlong Zi: [0000-0002-5133-4057](https://orcid.org/0000-0002-5133-4057)

Jie Wang: [0000-0003-4470-6171](https://orcid.org/0000-0003-4470-6171)

Zhong Lin Wang: [0000-0002-5530-0380](https://orcid.org/0000-0002-5530-0380)

Author Contributions

[#]H.Z., Y.Z., and X.H. contributed equally to this work.

Notes

The authors declare no competing financial interest.

■ ACKNOWLEDGMENTS

The authors gratefully acknowledge the support from the National Key Research and Development of China (Grant No. 2016YFA0202704), the “Thousands Talents” program for pioneer research and his innovation team in China, the National Natural Science Foundation of China (Grant Nos. S156114S021, S1432005, and S1372069), and the scholarship under the International Cultivation of Henan Advanced Talents. H.Z. and X.H. thank the China Scholarship Council for supporting research at the Georgia Institute of Technology.

■ REFERENCES

- (1) Zheng, L.; Lin, Z.-H.; Cheng, G.; Wu, W.; Wen, X.; Lee, S.; Wang, Z. L. Silicon-Based Hybrid Cell for Harvesting Solar Energy and Raindrop Electrostatic Energy. *Nano Energy* **2014**, *9*, 291–300.
- (2) Zheng, L.; Cheng, G.; Chen, J.; Lin, L.; Wang, J.; Liu, Y. S.; Li, H. X.; Wang, Z. L. A Hybridized Power Panel to Simultaneously Generate Electricity from Sunlight, Raindrops, and Wind around the Clock. *Adv. Energy Mater.* **2015**, *5*, No. 1501152.
- (3) Zi, Y.; Guo, H.; Wen, Z.; Yeh, M.-H.; Hu, C.; Wang, Z. L. Harvesting Low-Frequency (<5 Hz) Irregular Mechanical Energy: A Possible Killer Application of Triboelectric Nanogenerator. *ACS Nano* **2016**, *10*, 4797–4805.
- (4) Pancharoen, K.; Zhu, D.; Beeby, S. P. Temperature Dependence of a Magnetically Levitated Electromagnetic Vibration Energy Harvester. *Sens. Actuators, A* **2017**, *256*, 1–11.
- (5) Wang, X.; Wang, S. H.; Yang, Y.; Wang, Z. L. Hybridized Electromagnetic-Triboelectric Nanogenerator for Scavenging Air-Flow Energy to Sustainably Power Temperature Sensors. *ACS Nano* **2015**, *9*, 4553–4562.
- (6) Choi, M.; Murillo, G.; Hwang, S.; Kim, J. W.; Jung, J. H.; Chen, C. Y.; Lee, M. Mechanical and Electrical Characterization of PVDF-ZnO Hybrid Structure for Application to Nanogenerator. *Nano Energy* **2017**, *33*, 462–468.
- (7) Zhang, L.; Bai, S.; Su, C.; Zheng, Y. B.; Qin, Y.; Xu, C.; Wang, Z. L. A High-Reliability Kevlar Fiber-ZnO Nanowires Hybrid Nanogenerator and its Application on Self-Powered UV Detection. *Adv. Funct. Mater.* **2015**, *25*, 5794–5798.
- (8) Zhang, G. J.; Liao, Q. L.; Ma, M. Y.; Zhang, Z.; Si, H. N.; Liu, S.; Zheng, X.; Ding, Y.; Zhang, Y. A Rationally Designed Output Current Measurement procedure and Comprehensive Understanding of the Output Characteristics for Piezoelectric Nanogenerators. *Nano Energy* **2016**, *30*, 180–186.
- (9) Fan, F.-R.; Tian, Z.-Q.; Wang, Z. L. Flexible Triboelectric Generator. *Nano Energy* **2012**, *1*, 328–334.
- (10) Lin, L.; Wang, S. H.; Xie, Y. N.; Jing, Q. S.; Niu, S. M.; Hu, Y. F.; Wang, Z. L. Segmentally Structured Disk Triboelectric Nanogenerator for Harvesting Rotational Mechanical Energy. *Nano Lett.* **2013**, *13*, 2916–2923.

- (11) Li, A.; Zi, Y.; Guo, H.; Wang, Z. L.; Fernández, F. M. Triboelectric Nanogenerators for Sensitive Nano-Coulomb Molecular Mass Spectrometry. *Nat. Nanotechnol.* **2017**, *12*, 481–487.
- (12) Yang, Y.; Zhang, H. L.; Liu, R. Y.; Wen, X. N.; Hou, T. C.; Wang, Z. L. Fully Enclosed Triboelectric Nanogenerators for Applications in Water and Harsh Environments. *Adv. Energy Mater.* **2013**, *3*, 1563–1568.
- (13) Ma, M. Y.; Liao, Q. L.; Zhang, G.; Zhang, Z.; Liang, Q. J.; Zhang, Y. Self-Recovering Triboelectric Nanogenerator as Active Multifunctional Sensors. *Adv. Funct. Mater.* **2015**, *25*, 6489–6494.
- (14) Zhang, Q.; Liang, Q. J.; Liao, Q. L.; Yi, F.; Zheng, X.; Ma, M. Y.; Gao, F. F.; Zhang, Y. Service Behavior of Multifunctional Triboelectric Nanogenerators. *Adv. Mater.* **2017**, *29*, No. 1606703.
- (15) Chun, J.; Ye, B. U.; Lee, J. W.; Choi, D.; Kang, C.-Y.; Kim, S.-W.; Wang, Z. L.; Baik, J. M. Boosted Output Performance of Triboelectric Nanogenerator via Electric Double Layer Effect. *Nat. Commun.* **2016**, *7*, No. 12985.
- (16) Ahmed, A.; Hassan, I.; Mohammed, T. I.; Mostafa, H.; Reaney, I. M.; L. Koh, S. C.; Zu, J.; Wang, Z. L. Environmental Life Cycle Assessment and Techno-Economic Analysis of Triboelectric Nanogenerators. *Energy Environ. Sci.* **2017**, *10*, 653–671.
- (17) Wang, S. H.; Wang, Z. L.; Yang, Y. A One-Structure-Based Hybridized Nanogenerator for Scavenging Mechanical and Thermal Energies by Triboelectric–Piezoelectric–Pyroelectric Effects. *Adv. Mater.* **2016**, *28*, 2881–2887.
- (18) Gao, F. X.; Li, W. W.; Wang, X. Q.; Fang, X. D.; Ma, M. M. A Self-Sustaining Pyroelectric Nanogenerator Driven by Water Vapor. *Nano Energy* **2016**, *22*, 19–26.
- (19) Bae, J.; Li, J.; Kim, S.; Ha, J.; Li, B. S.; Park, Y.; Choong, C.; Kim, J. B.; Wang, Z. L.; Kim, H. Y.; Park, J. J.; Chung, U. I. Flutter-Driven Triboelectrification for Harvesting Wind Energy. *Nat. Commun.* **2014**, *5*, No. 4929.
- (20) Phan, H.; Phan, D. M.; Jeon, S. H.; Kang, T. Y.; Han, P.; Kim, G. H.; Kim, H. K.; Kim, K. H.; Wang, Y. H.; Hong, S. W. Aerodynamic and Aeroelastic Flutters Driven Triboelectric Nanogenerators for Harvesting Broadband Airflow Energy. *Nano Energy* **2017**, *33*, 476–484.
- (21) Yang, Y.; Zhang, H. L.; Zhu, G.; Lee, S.; Lin, Z. H.; Wang, Z. L. Flexible Hybrid Energy Cell for Simultaneously Harvesting Thermal, Mechanical, and Solar Energies. *ACS Nano* **2013**, *7*, 785–790.
- (22) Zabek, D.; Seunarine, K.; Spacie, C.; Bowen, C. Graphene Ink Laminate Structures on Poly(vinylidene difluoride) (PVDF) for Pyroelectric Thermal Energy Harvesting and Waste Heat Recovery. *ACS Appl. Mater. Interfaces* **2017**, *9*, 9161–9167.
- (23) Niu, S. M.; Wang, S. H.; Lin, L.; Liu, Y.; Zhou, Y. S.; Hu, Y. F.; Wang, Z. L. Theoretical Study of Contact-Mode Triboelectric Nanogenerators as an Effective Power Source. *Energy Environ. Sci.* **2013**, *6*, 3576–3583.
- (24) Wang, S. H.; Wang, X.; Wang, Z. L.; Ya, Y. Efficient Scavenging of Solar and Wind Energies in a Smart City. *ACS Nano* **2016**, *10*, 5696–5700.
- (25) Zhou, Y. S.; Wang, S. H.; Yang, Y.; Zhu, G.; Niu, S. M.; Lin, Z. H.; Liu, Y.; Wang, Z. L. Manipulating Nanoscale Contact Electrification by an Applied Electric Field. *Nano Lett.* **2014**, *14*, 1567–1572.
- (26) Kang, H.; Kim, H.; Kim, S.; Shin, H. J.; Cheon, S.; Huh, J. H.; Lee, D. Y.; Lee, S.; Kim, S. W.; Ho, J. H. Mechanically Robust Silver Nanowires Networks for Triboelectric Nanogenerators. *Adv. Funct. Mater.* **2016**, *26*, 7717–7724.
- (27) Zi, Y.; Lin, L.; Wang, J.; Wang, S.; Chen, J.; Fan, X.; Yang, P.-K.; Yi, F.; Wang, Z. L. Triboelectric–Pyroelectric–Piezoelectric Hybrid Cell for High-Efficiency Energy-Harvesting and Self-Powered Sensing. *Adv. Mater.* **2015**, *27*, 2340–2347.
- (28) Zhao, Z.; Pu, X.; Du, C.; Li, L.; Jiang, C.; Hu, W.; Wang, Z. L. Freestanding Flag-Type Triboelectric Nanogenerator for Harvesting High-Altitude Wind Energy from Arbitrary Directions. *ACS Nano* **2016**, *10*, 1780–1787.
- (29) Lee, J. H.; Lee, K. Y.; Gupta, M. K.; Kim, T. Y.; Lee, D. Y.; Oh, J.; Ryu, C.; Yoo, W. J.; Kang, C. Y.; Yoon, S. J.; Yoo, J. B.; Kim, S. W. Highly Stretchable Piezoelectric–Pyroelectric Hybrid Nanogenerator. *Adv. Mater.* **2014**, *26*, 765–769.
- (30) Yang, Y.; Jung, J. H.; Yun, B. K.; Zhang, F.; Pradel, K. C.; Guo, W. X.; Wang, Z. L. Flexible Pyroelectric Nanogenerators using a Composite Structure of Lead-Free KNbO₃ Nanowires. *Adv. Mater.* **2012**, *24*, 5357–5362.
- (31) Leng, Q.; Chen, L.; Guo, H. Y.; Liu, J. L.; Liu, G. L.; Hu, C. G.; Xi, Y. Harvesting Heat Energy from Hot/Cold Water with a Pyroelectric Generator. *J. Mater. Chem. A* **2014**, *2*, 11940–11947.
- (32) Quan, Z. C.; Han, C. B.; Jiang, T.; Wang, Z. L. Robust Thin Films-Based Triboelectric Nanogenerator Arrays for Harvesting Bidirectional Wind Energy. *Adv. Energy Mater.* **2016**, *6*, No. 1501799.
- (33) Zhang, Z.; Yao, C.; Yu, Y.; Hong, Z.; Zhi, M.; Wang, X. Mesoporous Piezoelectric Polymer Composite Films with Tunable Mechanical Modulus for Harvesting Energy from Liquid Pressure Fluctuation. *Adv. Funct. Mater.* **2016**, *26*, 6760–6765.
- (34) Garain, S.; Jana, S.; Sinha, T. K.; Mandal, D. Design of In Situ Poled Ce³⁺-Doped Electrospun PVDF/Graphene Composite Nanofibers for Fabrication of Nanopressure Sensor and Ultrasensitive Acoustic Nanogenerator. *ACS Appl. Mater. Interfaces* **2016**, *8*, 4532–4540.
- (35) Kepter, R. G.; Anderson, R. A. Piezoelectricity and Pyroelectricity in Polyvinylidene Fluoride. *J. Appl. Phys.* **1978**, *49*, 4490.
- (36) Xie, Y.; Wang, S.; Lin, L.; Jing, Q.; Lin, Z.-H.; Niu, S.; Wu, Z.; Wang, Z. L. Rotary Triboelectric Nanogenerator Based on a Hybridized Mechanism for Harvesting Wind Energy. *ACS Nano* **2013**, *7*, 7119–7125.
- (37) Yaqoob, U.; Uddin, A. S. M. I.; Chung, G. S. A Novel Tri-Layer Flexible Piezoelectric Nanogenerator Based on Surface-Modified Graphene and PVDF-BaTiO₃ Nanocomposites. *Appl. Surf. Sci.* **2017**, *405*, 420–426.
- (38) Proto, A.; Penhaker, M.; Bibbo, D.; Vala, D.; Conforto, S.; Schmid, M. Measurements of Generated Energy/Electrical Quantities from Locomotion Activities Using Piezoelectric Wearable Sensors for Body Motion Energy Harvesting. *Sensors* **2016**, *16*, 524.
- (39) Saravankumar, B.; Sooyon, S.; Kim, S. J. Self-Powered pH Sensor Based on a Flexible Organic–Inorganic Hybrid Composite Nanogenerator. *ACS Appl. Mater. Interfaces* **2014**, *6*, 13716–13723.
- (40) Wang, S.; Mu, X.; Yang, Y.; Sun, C.; Gu, A. Y.; Wang, Z. L. Flow-Driven Triboelectric Generator for Directly Powering a Wireless Sensor Node. *Adv. Mater.* **2015**, *27*, 240–248.
- (41) Quan, T.; Wang, X.; Wang, Z. L.; Yang, Y. Hybridized Electromagnetic-Triboelectric Nanogenerator for a Self-Powered Electronic Watch. *ACS Nano* **2015**, *9*, 12301–12310.
- (42) Xue, H.; Yang, Q.; Wang, D. Y.; Luo, W. J.; Wang, W. Q.; Lin, M. S.; Liang, D. L.; Luo, Q. M. A Wearable Pyroelectric nanogenerator and self-powered breathing sensor. *Nano Energy* **2017**, *38*, 147–154.
- (43) Chen, Y.; Wang, C.; Zhong, J.; Lin, S.; Xiao, Y.; Zhong, Q.; Jiang, H.; Wu, N.; Li, W.; Chen, S.; Wang, B.; Zhang, Y.; Zhou, J. Electrospun Polyetherimide Electret Nonwoven for bi-Functional Smart Face Mask. *Nano Energy* **2017**, *34*, 562–569.